Chapter 4: DATA PROCESSING AND ANALYSIS

4.1 Introduction

The intensity of ground vibration induced by blasting is critical in mining operations and produces several adverse effects on the surrounding environment and structures. Thus, the analysis and assessment of ground vibration are necessary to mitigate the damage and losses of structures and natural environments. Due to the complex nature of the earth's subsurface and other parameters such as geology, physical properties of rock mass, water reservoir, subsurface cavity, discontinuity, and lithology of rock mass, predicting and analyzing the strength of the blast-induced ground vibration is more challenging.

The intensity of the ground vibrations is quantitatively defined by the peak particle velocity (PPV) and dominant frequency. The PPV and dominant frequency are the most sensitive parameters for the prediction and assessment of BIGV and provide the appropriate results. Thus, several scientists and researchers have developed specific predictor model equations based on certain assumptions. These models depend mainly on the amount of explosive fired with a certain delay and observation distance from the blast site.

On the other hand, several countries try to establish their standard damage criteria of different structures to prevent the damage and losses due to ground vibration. In recent past studies, several algorithms such as ANN, FIS, SVM, ANN-PSO, ANN-ICA, MVRA, Fuzzy Logy, and FIM, etc., have been used to predict analysis of PPV and dominant frequency. The above algorithm depends mainly on two or more than two independent variable input parameters.

In the present ongoing study, orthogonal components like radial, transverse, vertical velocities as well as associated frequencies by using the super graphic software to determine the PPV, PVS, and dominant frequency, etc., have been considered for further analysis and interpretation. Acquired datasets processed through the different predictor models and algorithms for reasonable prediction and assessment to build events grid via configuration to

display on the monitor screen as shown in Figure 4.1, 4.2 and 4.3, respectively. The main objective of this chapter is to qualitative and quantitative analysis and interpretation of damage and non-damage circumstance for the structures present near the mine. To assess and analyze PPV, PVS, and dominant frequency, etc., the models used are attenuation predictor model equations, linear regression analysis, multivariate regression analysis (MVRA), and backpropagation artificial neural network. Several datasets from diverse disciplines are studied using the models indicated before in this study to fulfil the research goal.

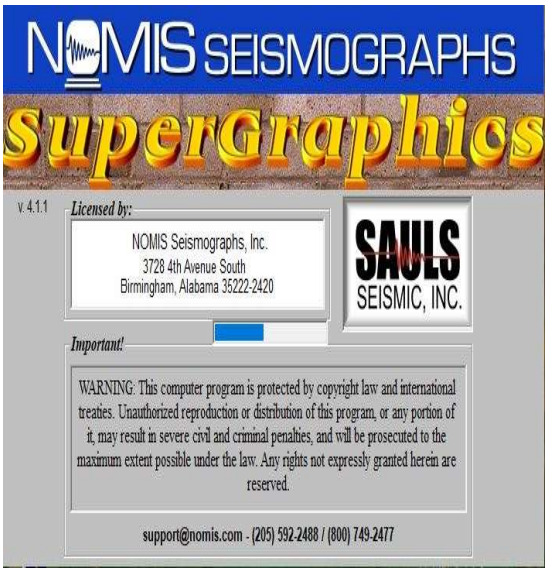

Figure 4.1Building event listening grid.

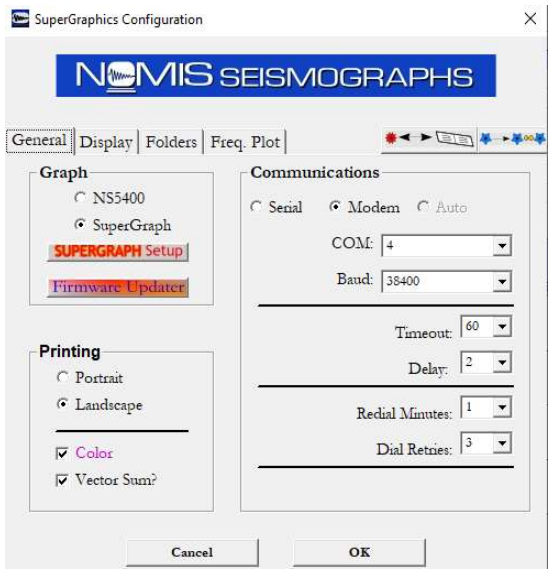

Figure 4.2 **C**onfiguration of building events.

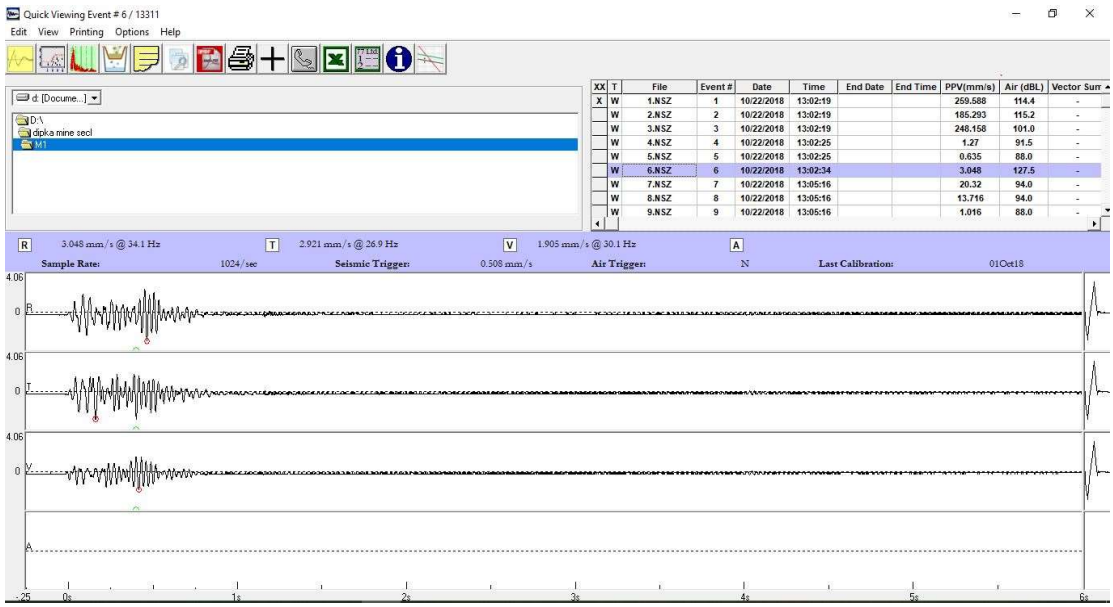

Figure 4.3 Building event display on the monitor screen.

4.2 Qualitative Damage Analysis of the Structures

According to the assumption, most structures present nearby the blasting sites are affected by cyclic induced ground vibrations. Initially, this repetition of ground vibration creates hairline cracks on the wall and roof of the structures and after that, it covert into large cracks. Finally, these structures undergo minor to moderate damage after a certain period. Therefore, the ground vibrations study is essential to minimize and prevent these damages to the structures due to ground vibrations.

Blasting energy also creates air overpressure and other physical effects such as; generation of dust clouds along with noxious fumes and fly rock. Dust cloud over the blasting site and cover over the region after the explosion is shown in Figures 4.4 and 4.5, respectively.

Five different mines have been covered for recording the ground vibrations and other associated parameters to achieve the objective of this study. The visual inspection was carried out in all five mines regarding various structures (mostly domestic structures) present nearby the mining areas and took photographs of these structures. After visualizing, many structures were found minor to major damage nearby mining areas. Therefore, the seismographs were installed near the present structures for this purpose, as shown in Figure 4.6. The visual analysis of plaster walls of different structures found the hairline cracks on the plaster wall at 200m from blast site, as shown in Figures 4.7 and 4.8, respectively. Whereas minor cracks were present on the wall of other plaster houses at 200m from blast site, as shown in figure 4.9. More cracks from hairline to minor levels on the same non-plaster wall of the brick-cement structure at 300m from blast site are shown in Figures 4.10 and 4.11. Photographs of major cracks on walls of two different non-plaster structures made up of brick-mud mortal at 250m from blast site are shown in Figures 4.12 and 4.13, respectively.

Over the five hundred blast event data were recorded in five different mines at a specific distance from the blast site to the last monitoring location. Most of the blast events data were

recorded nearby the present structures at a specific measured distance. Typical wavelets recorded in the same blast near the foundation of brick-cement mortar plaster wall structures located at the distance 510m, 520m and 530m from the blast site for the same amount of 324 kg of maximum charge per delay nearby structures are shown in Figure 4.14, 4.15, and 4.16 respectively. Typical wavelets recorded in other blasts near the foundation of a brick-cement mortar having non-plaster wall structure located at the distance of 430m and 490m from the blast site for the same amount of 420 kg of maximum charge per delay nearby structures are shown in Figures 4.17 and 4.18 respectively. Typical wavelets recorded in another blast near the foundation of a brick-mud mortal having non-plaster wall structure located at the distance of 425m and 440m from the blast site for the same amount of 470 kg of maximum charge per delay nearby structures are shown in Figures 4.19 and 4.20 respectively. The PPV and dominant frequency both play a key role in evaluating the intensity of ground vibration and damages to the structures. The damage levels are classified into four categories: threshold limits, cosmetic/hairline damage, minor damage, and major damage, listed in Table 4.1. Those structures oscillate under the threshold limits. There is no damage, and is a safe level of structures in the mining region (Singh et al. 2006).

Table 4.1: The classification of damage levels (Singh et al. 2006).

Classification	**Description of Damage**
Threshold Limits	Visually no cracks or deformation is present in the wall of the structures due to blasting vibrations
Cosmic or Hairline Damage	Loosing of paint; small plaster cracks at the joints between construction elements; initiation of hairline cracks, lengthening of old cracks on the walls.
Minor Damage	Loosening and falling of plaster; cracks in masonry around openings near partitions; hairline to 3mm cracks, fall of loss mortal or plaster.
Major Damage	Cracks of several millimetres in the wall; ruptures of opening vaults; structures weakening; fall of masonry; detachment of bricks from the wall, etc.

Figure 4.4 Dust cloud after the explosion.

Figure 4.5 Dust cover over the region.

Figure 4.6 Seismograph installed nearby the village.

Figure 4.7 A view of cosmetic/hairline crack on the plaster wall at 200m from blast site.

Figure 4.8 A view of cosmetic/hairline crack on the plaster wall at 200m from blast site.

Figure 4.9 A view of minor crack on the plaster wall at 200m from blast site.

Figure 4.10 A view of cosmetic/hairline to minor cracks on brick-cement wall at 300m from blast site.

Figure 4.11 A view of cosmetic/hairline to minor cracks on brick-cement wall of another house at 300m from blast site.

Figure 4.12 A view of minor to major cracks on the brick-mud mortar wall at 250m from blast site.

Figure 4.13 A view of major cracks on the non-plaster brick-mud mortar wall at 250m from blast site.

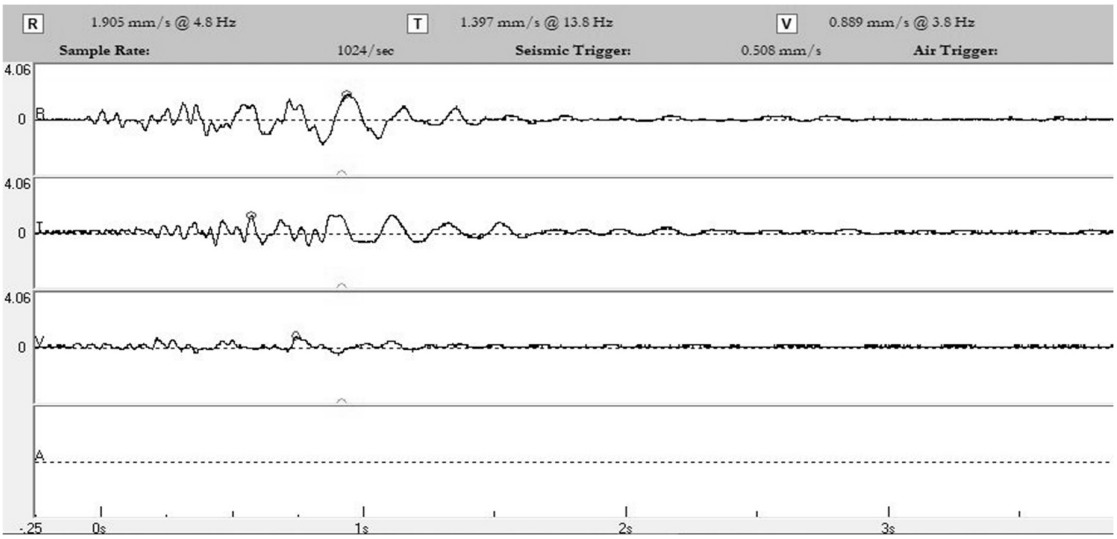

Figure 4.14 A typical wave signature recorded nearby the structure at 510m.

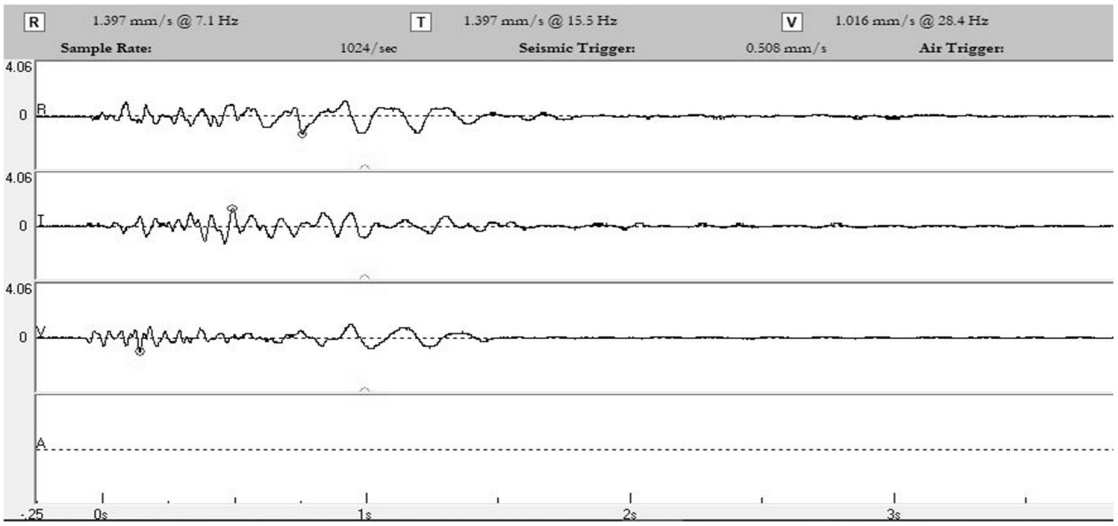

Figure 4.15 A typical wave signature recorded nearby the structure at 520m.

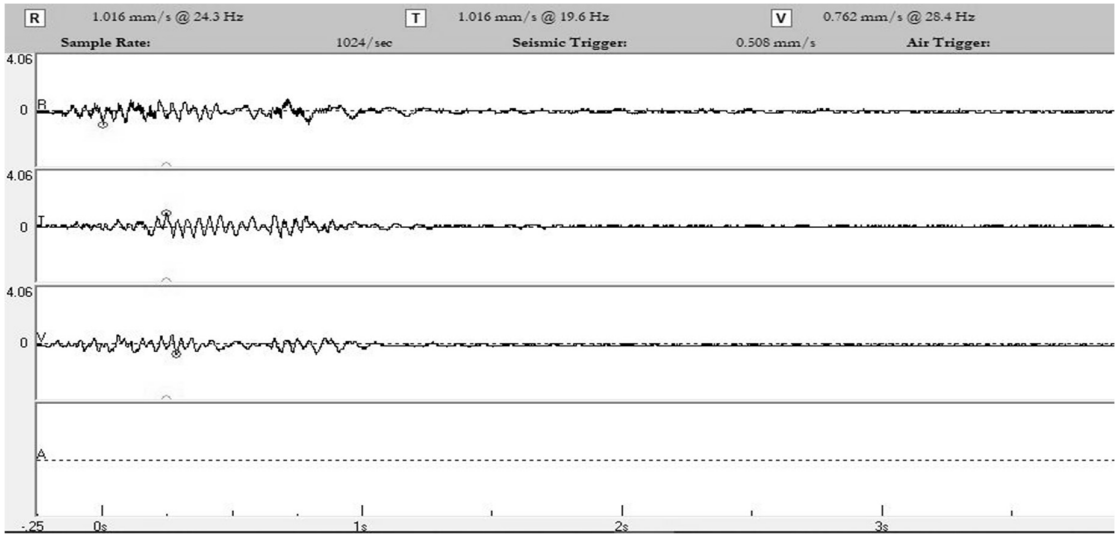

Figure 4.16 A typical wave signature recorded nearby the structure at 530m.

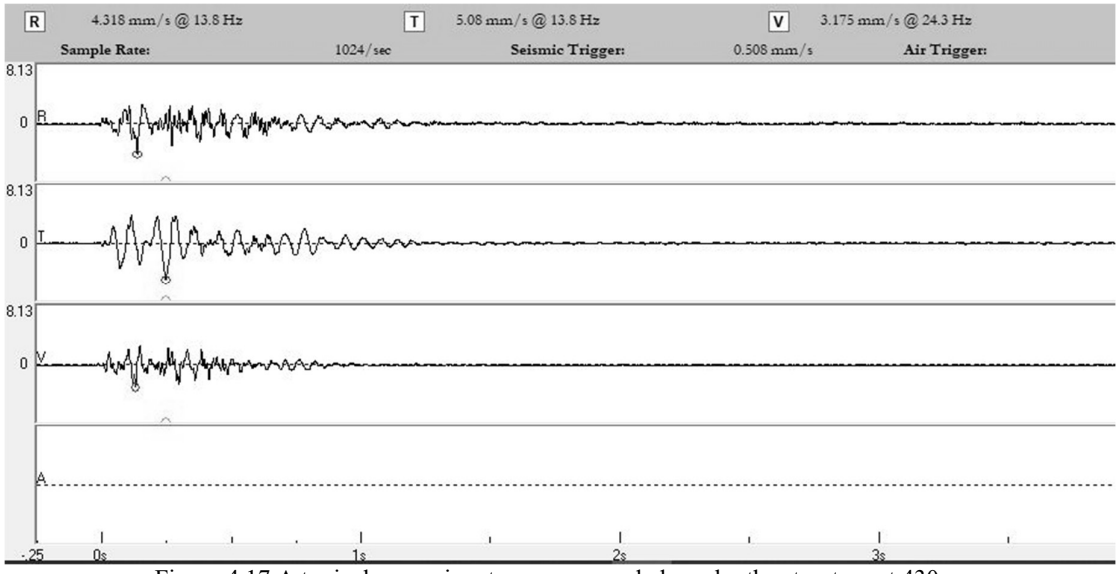

Figure 4.17 A typical wave signature was recorded nearby the structure at 430m.

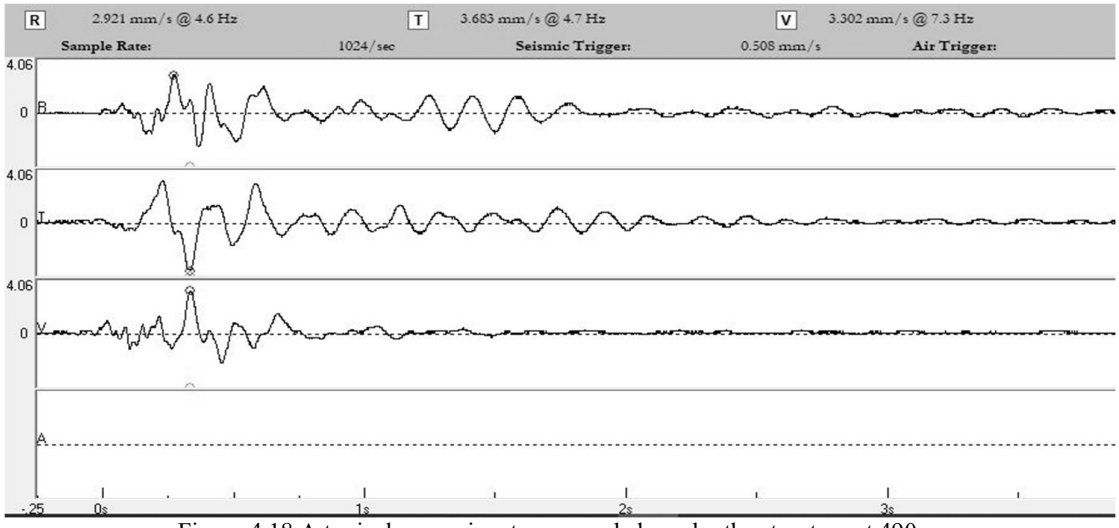

Figure 4.18 A typical wave signature recorded nearby the structure at 490m.

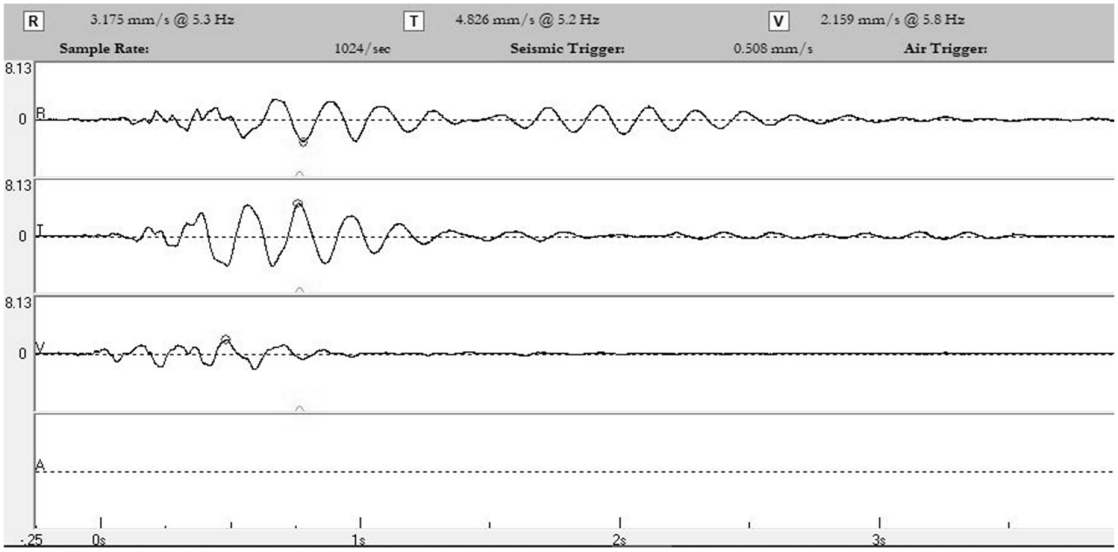

Figure 4.19 A typical wave signature was recorded nearby the structure at 425m.

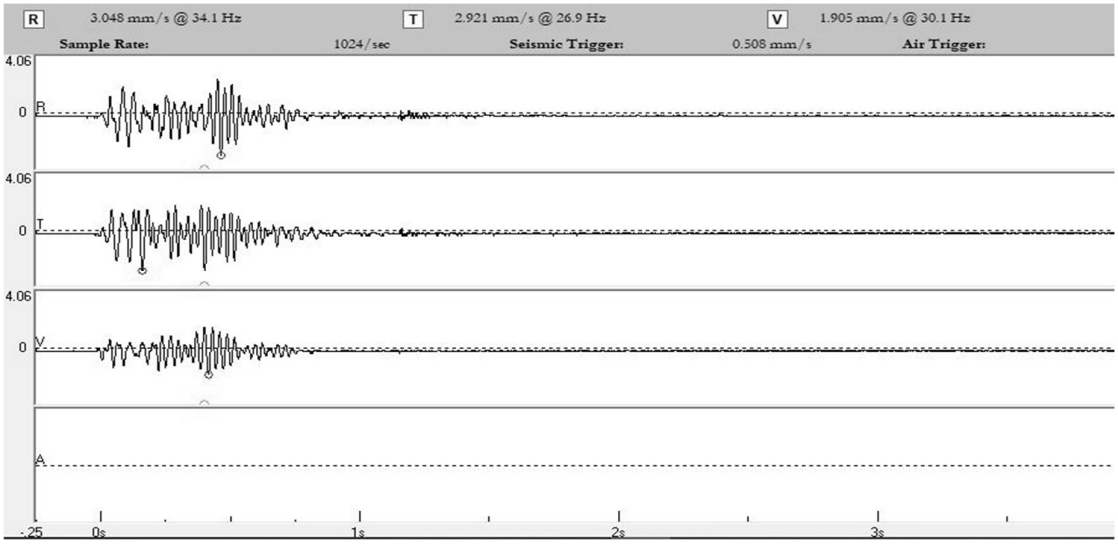

Figure 4.20 A typical wave signature was recorded nearby the structure at 440m.

4.3 Velocity Analysis

The most advanced seismographs were used to measure the component velocities such as radial, transverse, and vertical velocity as well as dominant frequency. These velocities play a key role to determine the magnitude of peak particle velocity for the desirable prediction and analysis of the intensity of ground vibration. In the processing of velocity analysis, picking the maximum amplitude among the three wavelets of component velocities is the PPV and is shown in the basic Equation (4.1). The orthogonal components such as radial,

transverse, and vertical velocities are measured in every blast event. On the other hand, the peak vector sum (PVS) is the square root of the sum of the square of radial, transverse, and vertical velocities, as shown in Equation (4.2).

$$PPV = k(D/\sqrt{Q})^{-b} \quad (4.1)$$

$$PVS = \sqrt{(R^2 + V^2 + T^2)} \quad (4.2)$$

4.4 Frequency Analysis

The ground vibration contains a wider range of frequency, which depends on the amount of explosive fired within a specific delay, geo-mining condition, and monitoring distance. However, the structures have their natural frequency under which it oscillates without any damage. When the frequency of ground vibration exceeds the natural frequency of structures, it undergoes damage. According to Medearis (1978), the natural frequency of structures varies from 4Hz to18Hz with its height and width. The frequency plays a key role in determining the level of damages. The amplitude of propagating seismic wave decays exponentially with dominant frequency and distance from the blast site in a homogeneous medium, as shown in Equation (4.3).

$$A = A_0 e^{-\pi f D/v q} \quad (4.3)$$

Where A, A_0 are amplitude of the seismic wave at monitoring distance D= D (m) and D= 0(m); f (Hz) is the dominant frequency of seismic wave velocity, v (m/s) with quality factor q. The datasets of dominant frequencies at various distances from the blast site at a certain specific maximum charge per delay (MCPD) are listed in Table 3.2. These data sets are processed through the super graphic software. These orthogonal frequency wavelets associated with the radial, transverse, and vertical ones are monitored in each blast event. The wavelets of orthogonal frequency components in radial, transverse, and vertical directions measured at various distances are shown in Figures 4.21, 4.22, 4.23 and 4.24, respectively.

The dominant frequency of the peak particle velocity should be obtained at the trigged time on the seismograph.

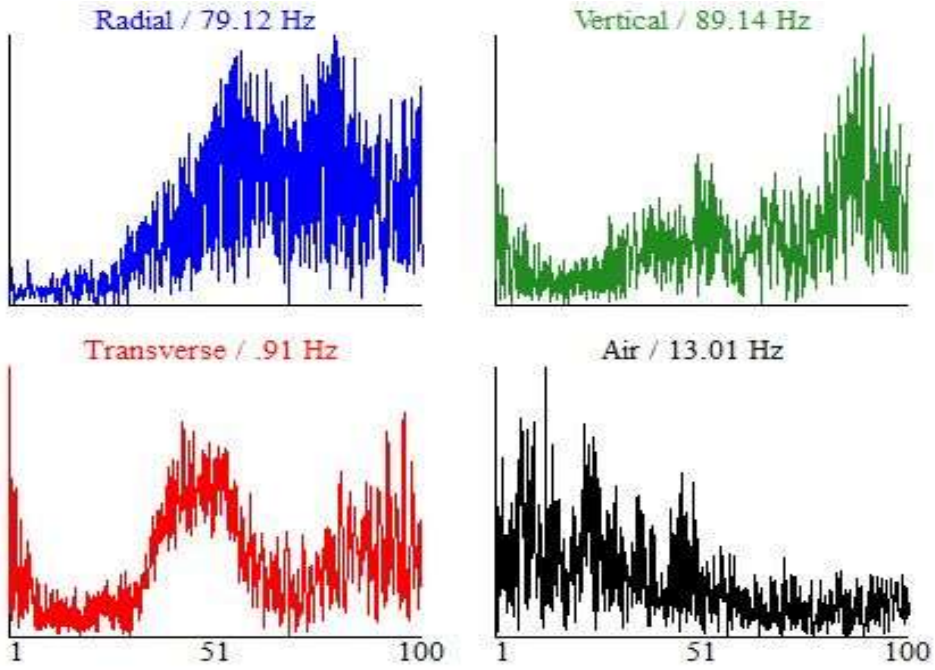

Figure 4.21 Frequency wavelets in orthogonal direction at 25m from the blast site.

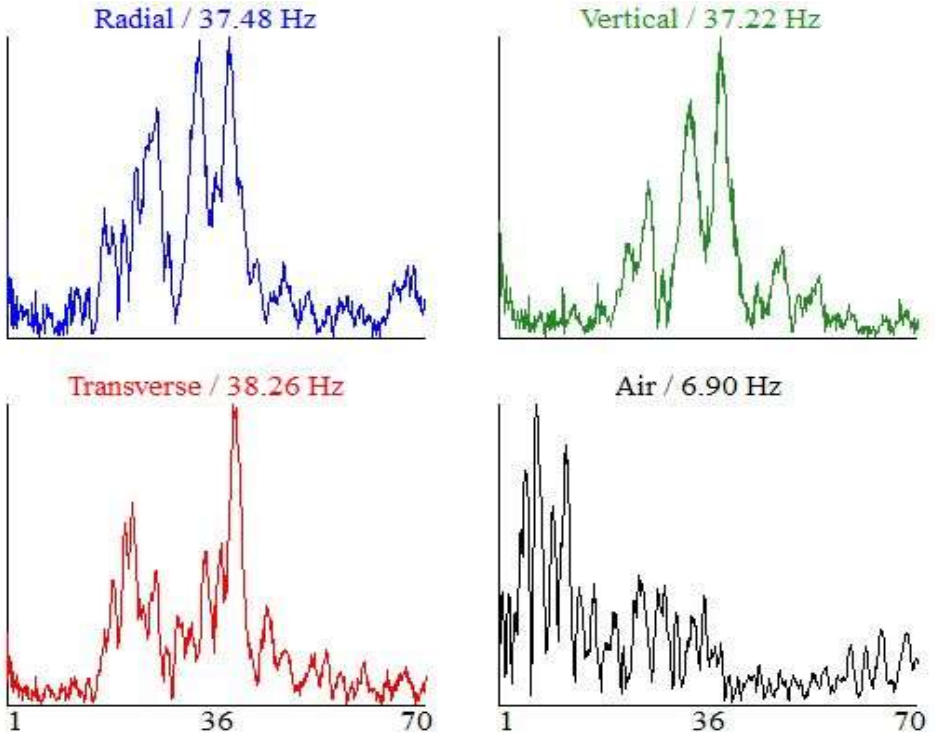

Figure 4.22 Frequency wavelets in orthogonal direction at 150m from the blast site.

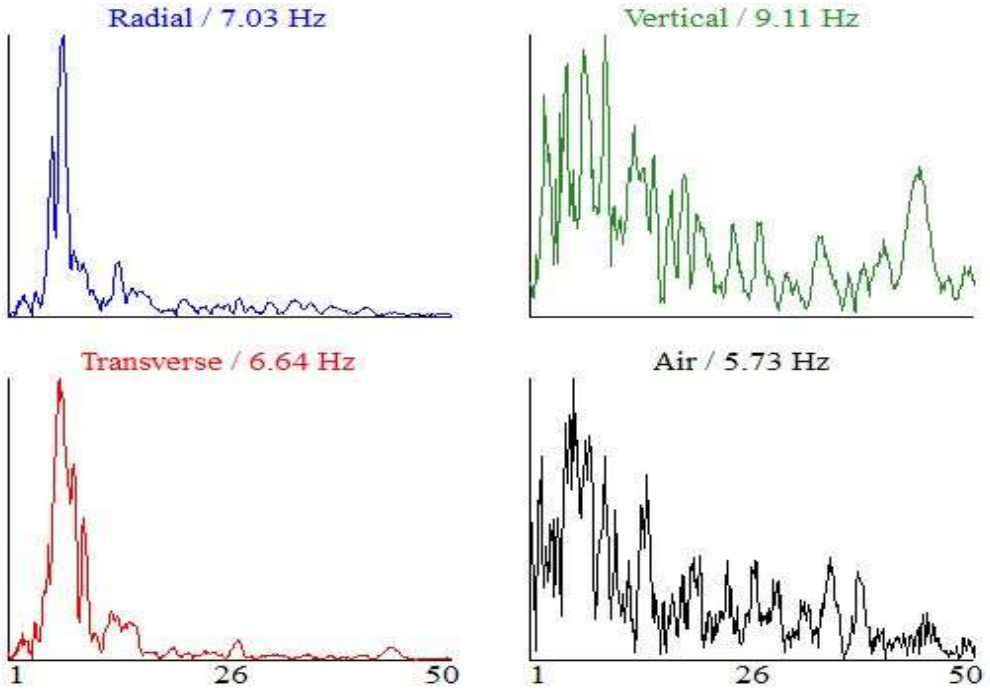

Figure 4.23 Frequency wavelets in orthogonal direction at 300m from the blast site.

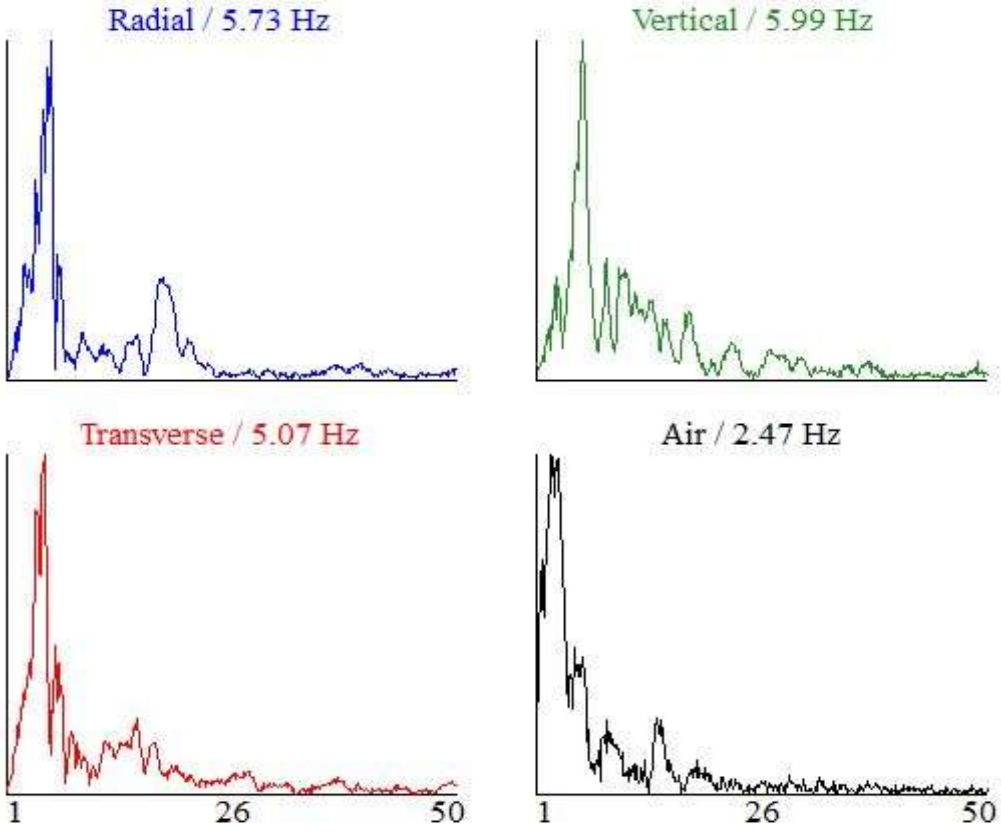

Figure 4.24 Frequency wavelets in orthogonal direction at 350m from the blast site.

4.5 Standard Limits for the Safe Level of Structures

Several scientists and researchers set the PPV values of different structures at a certain rate of dominant frequencies and proposed a model for the safety of structures. Initially, the United States Bureau of Mine (USBM) published RI 8507 model for ground vibration damage criteria which set the peak particle velocity (PPV) limits at dominant frequency. After that, several models were proposed for the safety of structures, such as OSM CFR 30 (USA), BS 7385 (British), Spanish standard, DIN 4150 (German), Indian Standard and some of them are listed in Table 2.4 to 2.7. The present study uses the structural response based on USBM and Indian model to establish the correlation between orthogonal component velocities and its associated dominant frequency at different distances. If the structures oscillate or vibrate under defined limits, structures should be safe.

4.5.1 Case I: Damage analysis of coal mine-1 Chhattisgarh

Structural response based on USBM RI 8507 model: The different datasets are processed through the given USBM RI 8507 model and define the damage criteria of present structures nearby mining area by plotting on a logarithmic scale. In the plotted diagrams, the Upper layer of the rhombus define permissible limits of drywall construction, and the lower layer of the rhombus define permissible limits of plaster and lath construction. The frequency and amplitude distribution are based on the USBM RI 8507 model. 24 datasets of six blast events in Table 3.2 are recorded and analyzed at different monitoring distances from blast site at 25m to 950m. A typical graph of frequency vs. amplitude plotted as 50m distance for R, T, and V is as shown in Figure 4.25 and other are included in appendix-A (from 4.26 to 4.42).

Structural response based on the Indian model: The same data set was taken as in previous USBM analysis to further analyze the Indian model for local structures by plotting on a logarithmic scale. The Indian model covers domestic, industrial, and historical structures and sensitive structures. The structural response describes the damage criteria by three individual

lines; continuous red line for domestic structures, blue break line for industrial structures, and black dotted line for historical and sensitive structures. The continuous red line for the medium structures such as domestic or non-commercial residential building like kuchcha, brick and cement houses, blue break line describes the permissible limit for strong structures such as industrial or commercial building and black dotted line describe permissible limit for the weak or old structures like historical and sensitive one. The frequency and amplitude distribution diagrams are plotted based on the Indian model. Similarly, 24 datasets of six blast event Table 3.2 are taken and analyzed at different monitoring distances from blast site from 25m to 950m. A typical graph of frequency vs. amplitude plotted as 50m distance for R, T, and V is as shown in Figure 4.43 and other are included in appendix-A (from 4.44 to 4.60).

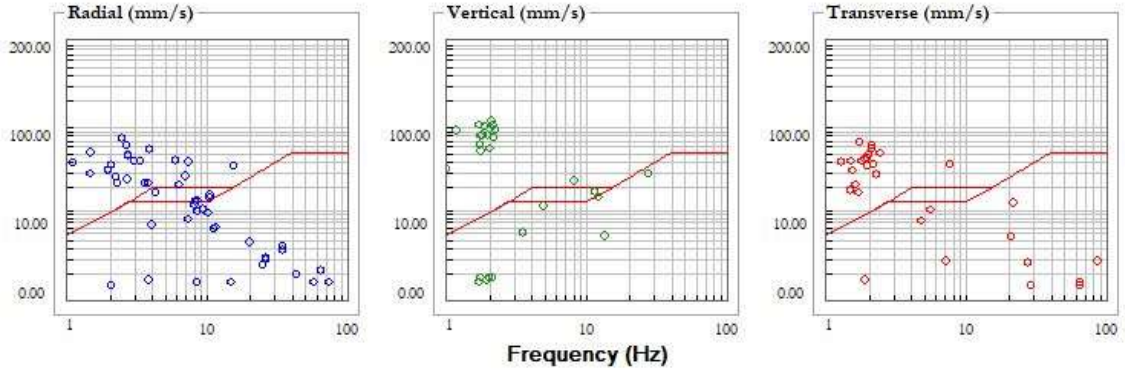

Figure 4.25 Frequency vs amplitude graph plotted at 50m distance.

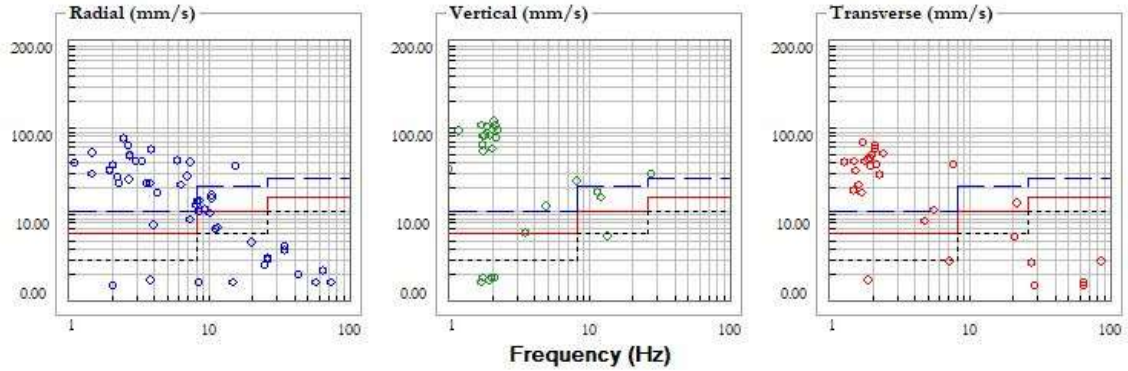

Figure 4.43 Frequency vs amplitude graph plotted at 50m distance.

4.5.2 Multivariate Regression Analysis (MVRA)

The multivariate regression analysis was carried out by choosing 40 datasets along with blasting parameters such as; monitoring distance, the maximum charge per delay, burden, spacing, number of blast holes, depth of holes, the diameter of the hole, powder factor, and total charge. The chosen data sets along with various blasting parameters, are utilized to determine the mathematical expressions for the peak particle velocity and dominant frequency. The expressions are used to predict the peak particle velocity, peak vector sum, and dominant frequency for given datasets. The derived models for the peak particle velocity PPV and dominant frequency **f** are given in Equations 4.4 and 4.5, respectively.

$$PPV = 30.17128-0.0097*D+0.05942* Q_{max} +0.0014144*TC+0.826352*TB+ 2.227614*B-0.72062*S-0.37704*NH-5.00792*HD+0.066992*HDI \quad (4.4)$$

$$Frequency\ (f) = 6.54903- 0.02968*D-0.02345* Q_{max} +0.00719*TC-0.15732*TB-47.2639*B+29.25495*S+0.534418*NH+15.3229*HD-0.26691*HDI \quad (4.5)$$

4.5.3 Back Propagation Artificial Neural Network Technique

Artificial neural network is an information processing system simulating the structure and Functions of the human brain. It is a highly interconnected structure that consists of many simple processing elements called neurons capable of performing massive parallel Computation data processing and representation. The neural network is first trained by processing a number of input data with the corresponding output. After collecting data from the various mines, a few datasets were analyzed through the backpropagation artificial neural network technique.

4.5.3.1 Network Training

Initially, a network needs to be trained before interpreting new information. Several Algorithms are available for the training of neural networks; however, the backpropagation algorithm is the most versatile and robust technique. It provides the most efficient learning

procedure for multilayer neural networks. Also, the fact that backpropagation algorithms are especially capable of solving predictive problems makes it so popular. Three layers' design backpropagation neural network BPNN architecture: the input layer contained nine neurons, the hidden layer contained seven neurons, and the output layer contained two neurons. Acquired datasets were applied to algorithm, training, testing, and validation for further analysis. The main goal is to achieve the actual output in terms of PPV and frequency after putting nine input blasting parameters on the backpropagation neural network technique. Its architectures are tabulated in Table 4.3.

To acquire the desired output, minimize the error between desired and obtained output. The input and output are connected with weights. The re-arrangement of weights is more complex and process is repeated until reached to desired output. Explained the process of re-arrangement of each weight to establish the expression by back propagation. Rearranged weight (new weight) $W_{5(}$new) is-

$$\mathrm{H1(in)} = \mathrm{X1} * \mathrm{W1} + \mathrm{X2} * \mathrm{W2} + \mathrm{b1}$$

$$\mathrm{H1(out)} = \frac{1}{1 + e^{-H1(in)}}$$

$$\mathrm{H2(in)} = \mathrm{X1} * \mathrm{W3} + \mathrm{X2} * \mathrm{W4} + \mathrm{b2}$$

$$\mathrm{H2(out)} = \frac{1}{1 + e^{-H2(in)}}$$

$$\mathrm{O1(in)} = \mathrm{H1(out)} * \mathrm{W5} + \mathrm{H2(out)} * \mathrm{W6} + \mathrm{b3}$$

$$\mathrm{O1(out)} = \frac{1}{1 + e^{-O1(in)}}$$

$$\frac{\delta \mathrm{E(Total)}}{\delta \mathrm{O1(out)}} = \mathrm{O1(out)} - \mathrm{O1(dout)}$$

$$\frac{\delta \mathrm{O1(out)}}{\delta \mathrm{Net(O1)}} = \mathrm{O1(out)} * \big(1 - \mathrm{O1(out)}\big)$$

$$\mathrm{Net(O1)} = \mathrm{H1(out)} * \mathrm{W5} + \mathrm{H2(out)} * \mathrm{W6} + \mathrm{b4}$$

$$\frac{\delta \mathrm{Net(O1)}}{\delta \mathrm{W5}} = \mathrm{H1(out)}\ \ Known\ value$$

$$W5(new) = \mathrm{W5} - \alpha * \frac{\delta \mathrm{E(Total)}}{\delta \mathrm{W5}}$$

$$W6(new) = \mathrm{W6} - \alpha * \frac{\delta \mathrm{E(Total)}}{\delta \mathrm{W6}}$$

Similarly we can have new weights like $W1_{(new)}$, $W2_{(new)}$, $W3_{(new)}$, $W4_{(new)}$…….

Where α- learning rate

E_{Total} - total error between desired and obtained output

4.5.3.2 Architecture of Datasets

The backpropagation neural network technique is adopted at this moment as this architecture is the most suitable for identifying the problem and providing its best solution. The main objective of this analysis is to predict the peak particle velocity and dominant frequency for the respective blasting parameters such as depth of holes, the diameter of holes, spacing, burden, total charge, total booster, the maximum charge per delay, number of holes and monitoring distance. The nomenclature of network architecture is given in Table 4.2.

Table 4.2: The network architecture.

1	Number of input neurons	9
2	Number of output neurons	2
3	Number of hidden layers	1
4	Number of hidden neurons	7
5	Number of training epochs	562
6	Number of training datasets	198
7	Number of testing datasets	18
8	Error goal	0.009

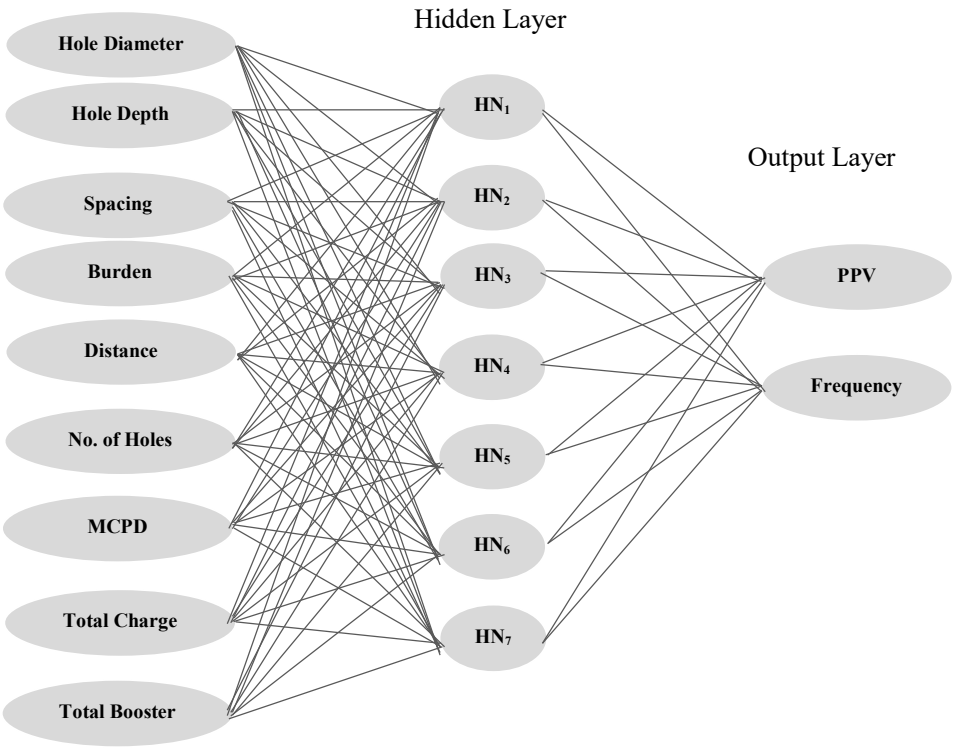

Figure 4.61 Backpropagation neural network configuration.

4.6 Surface Coal Mine

4.6.1 Case II: Damage analysis of coal mine-2 Madhya Pradesh

Structural response based on the Indian model: The performance data of mine-2 for further analysis to the Indian model for local structures by a graph plotting on a logarithmic scale. The Indian model covers domestic, industrial, and historical structures and sensitive structures. The structural response describes the damage criteria by three individual lines; continuous red line for domestic structures, blue break line for industrial structures, and black dotted line for historical and sensitive structures. The frequency and amplitude distribution diagrams are plotted based on the Indian model. Similarly, 28 datasets of seven blast events of Table 3.8 were taken and analyzed at different monitoring distances from the blast site from 50m to 1400m. A typical graph of frequency vs. amplitude plotted as 50m distance for

R, T, and V is as shown in Figure 4.62 and other are included in appendix-A (from 4.63 to 4.81).

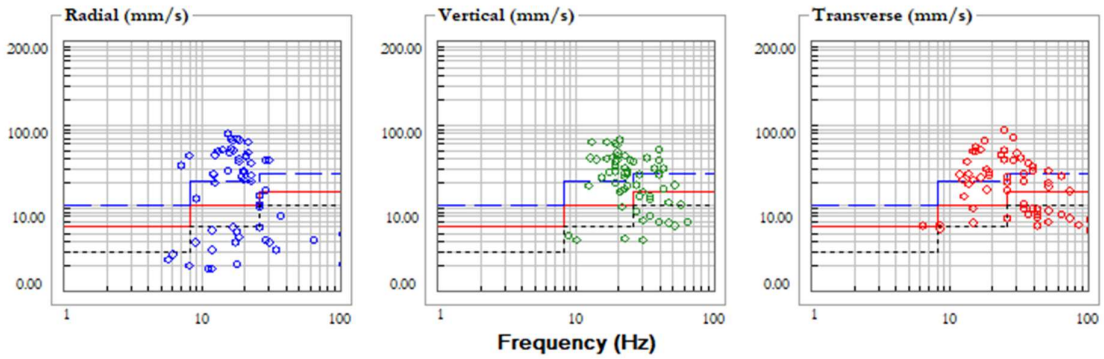

Figure 4.62 Frequency vs amplitude graph plotted at 50m distance.

4.6.2 Site Specific Constant

The site-specific constant is helpful to establish a relationship between the measured and predicted value of PPV. The site-specific constants are determined using the linear regression analysis, and it varies from mine to mine site due to the physical properties of the rock mass. The derived site-specific constants should be applied on a particular mine site only. The site-specific constants such as k, b, and a are determined for a particular mine is tabulated in Table 4.3.

Table 4.3: The site-specific constants

References	k	b	a
Duvall-Petkof (1959)	440.25	1.6797	……
Langefors-Kihlstrom (1963)	0.11223	-2.716	…….
General predictor 1964	562.50	1.69	0.81
Ambraseys-Hendron (1968)	3449.05	1.7358	……
Indian Standard (DGMS) 1983	0.11223	-1.358	……

4.6.3 Attenuation Model Equation

Several scientists and researchers have developed their attenuation equations or models to predict PPV. Attenuation models depend mainly on maximum charge per delay and monitoring distance from the blast site and site-specific constants. In the present study, 46

datasets are taken from table 3.8 and are used to predict and interpret through the applied attenuation equations. Depending on the attenuation equations, site-specific constants maybe two or more than two. The prediction of the intensity of blast-induced ground vibrations was carried out by different attenuation predictor models for five various mines. In the present study, five various predictor equations are used to predict the PPV along with the Indian predictor equation provided by DGMS. The basic attenuation Equation (4.6) is as follows-

$$PPV = k(SD)^{-b} \quad (4.6)$$

$$\log PPV = \log k + (-b)\log SD$$

Where k and b are the site-specific constant of rock mass and SD is scaled distance

4.6.3.1 Predicted by Duvall-Petkof

$$\mathbf{V} = 440.25(\mathbf{SD})^{-1.6797} \quad (4.7)$$

The attenuation Equation (4.7) becomes complete to establish the relationship between predicted PPV and scaled distance (SD) functions of maximum charge per delay and monitoring distance from the blast site. The site-specific constants **k = 440.25** and **b = -1.6797** are determined using regression analysis by plotting between SD and measured PPV on a logarithmic scale.

4.6.3.2 Predicted by Langefors-Kihlstrom

$$PPV = 0.1122(\mathbf{SD})^{1.358} \quad (4.8)$$

The attenuation Equation (4.8) becomes complete to establish the relationship between predicted PPV and scaled distance (SD) functions of maximum charge per delay and monitoring distance from the blast site. The site constants **k = 0.1123** and **b = 2.716** are determined using regression analysis by plotting between SD and PPV on a logarithmic scale.

4.6.3.3 Predicted by General Predictor

$$PPV = 566.50\ \mathbf{D}^{-1.69}\ \mathbf{Q}^{0.8105} \quad (4.9)$$

The attenuation Equation (4.9) becomes complete to establish the relationship between predicted PPV and scaled distance (SD) functions of maximum charge per delay and monitoring distance from the blast site. The site constants **k = 566.50** and **b = -1.69**, and **a = 0.8105** are determined using regression analysis by plotting between SD and measured PPV on a logarithmic scale

4.6.3.4 Predicted by Ambraseys-Hendron

$$PPV = 3449.25\ (\mathbf{SD})^{-1.7358} \quad (4.10)$$

The Equation (4.10) becomes complete to establish the relationship between predicted PPV and scaled distance (SD) is the maximum charge per delay and monitoring distance from the blast site. The site constants **k =3449.25** and **b= 1.7358** are determined using regression analysis by plotting between SD and PPV on a logarithmic scale.

4.6.3.5 Predicted by Indian Standard

$$PPV = 0.1122(\mathbf{SD})^{1.358} \quad (4.11)$$

The attenuation Equation (4.11) becomes complete to establish the relationship between predicted PPV and scaled distance (SD) is the maximum charge per delay and monitoring distance from the blast site. The site constants **k = 0.1122** and **b = 1.358** are determined using regression analysis by plotting between SD and PPV on a logarithmic scale.

4.7 Stone Quarry

4.7.1 Case III: Damage analysis of limestone quarry-3 Chhattisgarh

Structural response based on Indian model: The performance of data of limestone quarry-3 for further analysis to Indian model for local structures by a graph plotting on a logarithmic scale. The Indian model covers domestic, industrial, and historical structures and sensitive structures. The structural response describes the damage criteria by three individual lines; continuous red line for domestic structures, blue break line for industrial structures, and black

dotted line for historical and sensitive structures. The amplitude versus associated frequency distribution diagrams is plotted based on the Indian model. Similarly, 28 datasets of seven blast events in Table 3.13 were taken and analyzed at different monitoring distances from the blast site from 50m to 1400m. A typical graph of frequency vs. amplitude plotted as 50m distance for R, T, and V is as shown in Figure 4.82 and other are included in appendix-A (from 4.83 to 4.101).

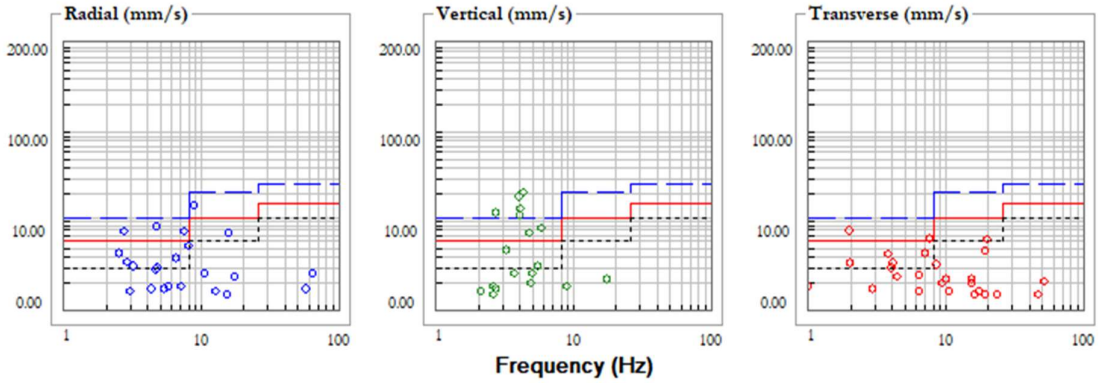

Figure 4.82 Frequency vs amplitude graph plotted at 50m distance.

4.7.2 Case IV: Damage analysis of stone quarry-4 Bihar

Structural response based on the Indian model: The performance of data sets of stone quarry-4 for further analysis to the Indian model for structures by a graph plotting on a logarithmic scale. The Indian model covers domestic, industrial, and historical structures and sensitive structures. The structural response describes the damage criteria by three individual lines; continuous red line for domestic structures, blue break line for industrial structures, and black dotted line for historical and sensitive structures. The frequency and amplitude distribution diagrams are plotted based on the Indian model. Similarly, 28 datasets of seven blast events in Table 3.14 were taken and analyzed at different monitoring distances from the blast site from 50m to 1400m. A typical graph of frequency vs. amplitude plotted as 50m distance for R, T, and V is as shown in Figure 4.102 and other are included in appendix-A (from 4.103 to 4.121).

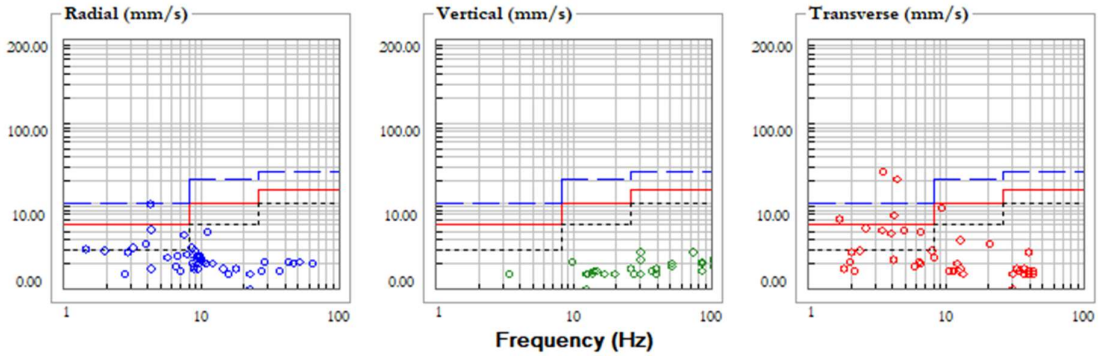

Figure 4.102 Frequency vs amplitude graph plotted at 50m distance.

4.7.3 Case V: Damage analysis of stone quarry-5 Uttar Pradesh

Structural response based on Indian model: The performance of data sets of stone quarry-5 data sets for further analysis to the Indian model for local structures by a graph plotting on a logarithmic scale. The Indian model covers domestic, industrial, and historical structures and sensitive structures. The structural response describes the damage criteria by three individual lines; continuous red line for domestic structures, blue break line for industrial structures, and black dotted line for historical and sensitive structures. The amplitude versus associated frequency distribution diagrams is plotted based on the Indian model. Similarly, 28 datasets of seven blast events in Table 3.17 were taken and analyzed at different monitoring distances from the blast site from 50m to 1400m. A typical graph of frequency vs. amplitude plotted as 50m distance for R, T, and V is as shown in Figure 4.122 and other are included in appendix-A (from 4.123 to 4.141).

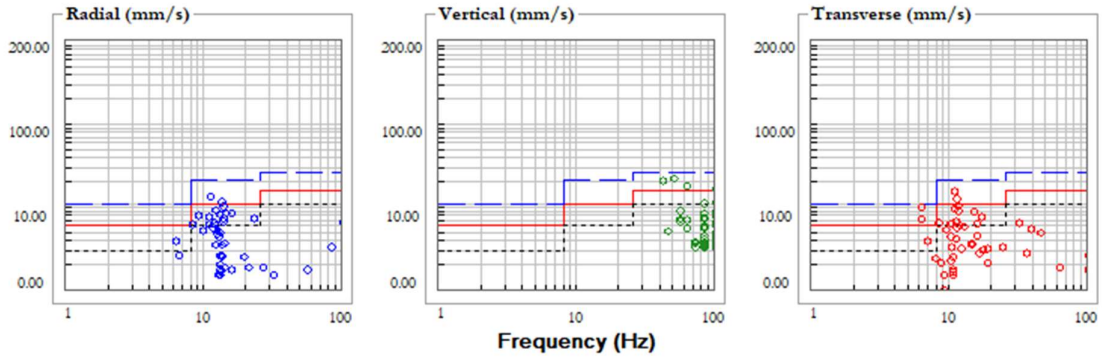

Figure 4.122 Frequency vs amplitude graph plotted at 50m distance.